HEAT EXCHANGE BETWEEN A HORIZONTAL CYLINDER AND THREE-PHASE FLUIDIZED BED

V. S. Belousov, L. K. Vasanova, V. V. Korotke, A. V. Sokolov, and G. P. Yasnikov

UDC 536.24:66.047.01

Results are presented of theoretical and experimental studies of heat exchange between a liquid fluidized bed through which air bubbles pass and a horizontal cylinder.

The intensification of heat exchange with the passage of gas bubbles through a liquid fluidized bed can be explained by additional convective dispersion due to wave motions of the liquid, which are caused by variations of the volume and shape of the surfacing bubbles [1, 2]. Dependences of the coefficients of convective dispersion (thermal diffusivity) and heat exchange on gas volume were established earlier [2]:

$$D = k_D \left(\frac{\beta}{1-\beta}\right)^{1/6}, \quad \mathrm{St}_\beta = k_s \mathrm{St} \left(\frac{\beta}{1-\beta}\right)^{1/12}. \tag{1}$$

Rigorous analytic solutions of problems of external exchange in a disperse bed were obtained earlier [3, 4]. The approaches developed then are used below for analysis of external heat exchange in a three-phase fluidized bed. Since, because of their complexity, it is impossible at the present time to obtain analytic solutions of these problems, therefore it is entirely reasonable to use approximation and estimation methods based on model equations [5] with the results corrected on the basis of experimental data.

Following our earlier work [3, 4], we shall the heat exchange of a horizontal cylinder with a bed in a single-phase approximation using the equation of convective thermal conductivity [4]

$$(\mathbf{u}\nabla)\, T = \nabla(\hat{a}\nabla T) - k_q T,$$
$$\hat{a} = \hat{\lambda}/\rho_0 c_0; \quad T = \frac{t - t_0}{t_w - t_0} = \frac{\vartheta_0}{\vartheta_w} \tag{2}$$

with boundary conditions

$$T_{r\to\infty} = 0; \quad T_0 + \frac{\lambda}{\alpha}\left(\frac{\partial T}{\partial n}\right)_w = T_w; \quad \frac{q}{\lambda} = -\left(\frac{\partial T}{\partial n}\right)_w.$$

With the aid of von Mises transformations [6], it is convenient to move in (2) to a coordinate system that is related to the heat-exchange surface such that the y-axis is oriented along the normal to the surface and the x-axis is oriented from the head point of the cylinder along the line of its intersection with the plane perpendicular to the axis:

$$\frac{R+y}{R} u_y \frac{\partial T}{\partial y} + u_x \frac{\partial T}{\partial x} = \frac{R}{R+y} \frac{\partial}{\partial x}\left(a_\parallel \frac{\partial T}{\partial x}\right) + \frac{\partial}{\partial y}\left(a_\perp \frac{R+y}{R} \frac{\partial T}{\partial y}\right) - k_q T. \tag{3}$$

For an infiltrated granular bed, the principal values $a_\parallel$ and $a_\perp$ of the thermal-diffusivity tensor were given earlier [4].

S. M. Kirov Ural Polytechnic Institute, Ekaterinburg. Translated from Inzhenerno-fizicheskii Zhurnal, Vol. 62, No. 2, pp. 180-187, February, 1992. Original article submitted May 13, 1991.

 1062-0125/92/6202-0128$12.50

The experimentally studied fluidization regimes are characterized by high Peclet numbers ($\sim 10^3$-10^4), and the heat-exchange process is self-similar with respect to the size of the cylinder. Therefore, T differs from zero in a thin boundary layer, and the variation of T with respect to y is greater than along the x-axis [4]. Taking these circumstances into account, ignoring $\partial T/\partial x$, and assuming $a_\perp = a$ and $\mathbf{u} = \{u_x, u_y\} = \{u, 0\}$, we obtain from (3) an equation [4] for a plate, which, according to the concepts introduced by Dil'man and Polyanin [5], can be considered a model equation for our problem:

$$u\frac{\partial T}{\partial x} = \frac{\partial}{\partial y}\left(a\frac{\partial T}{\partial y}\right) - k_q T, \tag{4}$$

$$T_{y\to\infty} = 0, \quad T_{y=0} = 1. \tag{5}$$

We use an algebraic method [5] to analyze problem (4) and (5). First, we shall examine a flow with a constant filtration velocity and a constant thermal diffusivity

$$u = u_0 = \text{const}, \quad a = a_0(1+\gamma); \quad \gamma = k\frac{\ell u}{a_0}, \tag{6}$$

where γ has the meaning of a "microstructural" Péclet number. A rigorous solution of this problem was obtained earlier [4]. The characteristic "microscale" ℓ is equal to the particle radius, and k = 0.38. We take the length of the plate L as the "macroscopic" scale. Introducing the dimensionless variables x/L and y/L (which we shall denote by the same letters x and y), we transform (4) and the thermal flux [see (2)] to dimensionless form:

$$\mathrm{Pe}_0\frac{\partial T}{\partial x} = (1+\gamma)\frac{\partial^2 T}{\partial y^2} - \frac{k_q L^2}{a_0}T, \tag{7}$$

$$\mathrm{St} = \frac{1+\gamma}{\mathrm{Pe}_0}\left(\frac{\partial T}{\partial y}\right)_w, \quad \mathrm{Pe}_0 = \frac{u_0 L}{a_0}, \quad \mathrm{St} = \frac{q}{\rho_0 c_0 \vartheta_0 u_0}. \tag{8}$$

According to Dil'man and Polyanin [5], in (7) we extend the y coordinate as follows:

$$y = \frac{(1+\gamma)}{\mathrm{St}\,\mathrm{Pe}_0}\xi, \tag{9}$$

such that $(\partial T/\partial \xi)_w = -1$, then,

$$\frac{(\mathrm{St}\,\mathrm{Pe}_0)^2}{1+\gamma}\left\{\frac{\partial^2 T}{\partial \xi^2}\right\} - \mathrm{Pe}_0\left\{\frac{\partial T}{\partial x}\right\} - \frac{k_q L^2}{a_0}\{T\} = 0. \tag{10}$$

We move from differential Eq. (10) to an algebraic equation for the average Stanton number by substituting constants (± 1) for the quantities in the braces [5]:

$$\mathrm{St}^2 - \frac{(1+\gamma)}{\mathrm{Pe}_0} - \frac{(1+\gamma)}{\mathrm{Pe}_0^2}\frac{k_q L^2}{a_0} = 0. \tag{11}$$

In the model in question, as applied to a fluidized bed, the role of heat sinks is played by solid particles that enter the wall zone, where the temperature gradient from the bed is concentrated. The sinks can, in principle, be of a different nature. We shall examine in (11) two limiting cases: $k_q \to 0$ and $k_q \to \infty$. For $k_q \to 0$, from (11) we find

$$\mathrm{St} \xrightarrow[k_q\to 0]{} \mathrm{St}_0 = \sqrt{\frac{1+\gamma}{\mathrm{Pe}_0}}, \quad q_0 = \rho_0 c_0 \vartheta_0 \sqrt{\frac{(1+\gamma)a_0 u_0}{L}}, \tag{12}$$

and for $k_q \to \infty$ we have

$$\mathrm{St} \xrightarrow[k_q\to\infty]{} \mathrm{St}_\infty = \sqrt{\frac{(1+\gamma)a_0 k_q}{u_0^2}}, \quad q_\infty = \rho_0 c_0 \vartheta_0 \sqrt{(1+\gamma)a_0 k_q}. \tag{13}$$

The expression for q_∞ coincides with the exact analytic result obtained earlier [4], while q_0 differs from the exact result [4]

$$q_0 = \rho_0 c_0 \vartheta_0 \frac{2}{\sqrt{\pi}}\sqrt{\frac{(1+\gamma)a_0 u_0}{L}} \tag{14}$$

by the factor $2/\sqrt{\pi} \approx 1.13$.

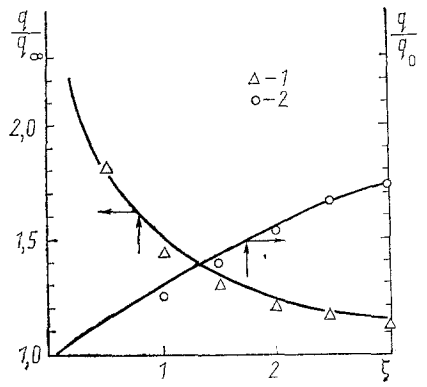

Fig. 1. Ratios of average thermal flux to limiting values: 1) q/q_∞; 2) q/q_0 versus dimensionless length ζ. The solid curves represent exact calculations [4] and the points indicate approximations by (16).

Expressing the last two terms in (11) by St_0 and St_∞, which were obtained from the exact formulas for q_0 and q_∞, we arrive at an asymptotically corrected equation for St:

$$St^2 - \frac{\pi}{4} St_0^2 - St_\infty^2 = 0. \tag{15}$$

Let us estimate the accuracy of (15). Taking (13) and (14) into account in (15), we find

$$\frac{q}{q_\infty} = \sqrt{\frac{\zeta+1}{\zeta}}; \quad \frac{q}{q_0} = \sqrt{\frac{\pi}{4}}\sqrt{1+\zeta}, \quad \zeta = \frac{k_q L}{u_0}. \tag{16}$$

The results of calculations of q/q_∞ and q/q_0 by the exact formulas [4] and approximate formulas (16) are presented in Fig. 1. As can be seen from the graphical comparison, Eq. (15) describes fairly accurately the heat exchange for intermediate values of k_q [7].

If there are no exact analytic asymptotics, the relations obtained by the methods of Dil'man and Polyanin [5] can be corrected on the basis of experimental data. This is especially important for the development of engineering methods for the calculation of processes of heat and mass transfer in complex systems – for example, three-phase fluidized beds. Numerical estimates based on experimental data for a fluidized bed show that the last term, which takes into account heat absorption in the boundary layer by particles (sinks), is negligible, but asymptotics (12) do not work in this case.

Let us examine first a fluidized bed without gas bubbles. As earlier [4], we shall use an approximation of a thin boundary layer. Assuming $k_q = 0$ in (4) and introducing the self-similar variable $\eta = y/\delta(x)$ [$T = T(\eta)$], we transform (4) to

$$\frac{\partial^2 T}{\partial \eta^2} + \left(\frac{u\delta}{a}\frac{\partial \delta}{\partial x}\right)\eta\frac{\partial T}{\partial \eta} + \left(\frac{1}{a}\frac{\partial a}{\partial \eta}\right)\frac{\partial T}{\partial \eta} = 0. \tag{17}$$

At a = const, (17) becomes the earlier equation [4] for stationary flow past a plate. Analysis of this equation by the algebraic method naturally leads to the above-derived relations (12), (13), (15), and (16).

Using the relationship between the thicknesses of the thermal δ^* and hydrodynamic δ boundary layers [8]

$$\delta^* = f^*(\mathrm{Pr})\,\delta \text{ and } u = u_0 f(\eta) = (u_0/f^{*m})\,\eta^m,$$

and taking relation (8) into account, from (6) we obtain

$$\frac{\partial a}{\partial \eta} = kl\frac{\partial u}{\partial \eta} = klu_0\frac{\partial f}{\partial \eta} = \frac{mklu_0}{f^{*m}}\eta^{m-1}. \tag{18}$$

In addition, with intense particle mixing, it can be assumed that the convective mechanism of heat transfer predominates. Therefore, $\gamma \gg 1$, $a = k\ell u = (k\ell u_0/f^{*m})\eta^m$ in (6). Taking this circumstance and (18) into account, we represent the last term in (17) as

$$\frac{1}{a}\frac{\partial a}{\partial \eta}\frac{\partial T}{\partial \eta} = \frac{m}{\eta}\frac{\partial T}{\partial \eta}. \tag{19}$$

For flow of an incompressible medium with solid particles past a plate, we have [9]

$$\frac{\delta^*}{x} = A\,\mathrm{Re}_x^{-0,2} = A\left(\frac{u_0}{\nu_0}\right)^{-0,2} x^{-0,2}, \tag{20}$$

hence,

$$\frac{\partial\delta^*}{\partial x} = 0{,}8\,\frac{\delta^*}{x} = f^*(\mathrm{Pr})\,\frac{\partial\delta}{\partial x}. \tag{21}$$

Since δ^*/x varies insignificantly [9], and considering the subsequent correction of the results, we substitute $\delta^*(\ell)/\ell$ for δ^*/x in (21):

$$\frac{\partial\delta}{\partial x} = 0{,}8\,\frac{\delta^*}{xf^*} \approx \frac{0{,}8}{f^*}\,\frac{\delta^*}{l} = \frac{0{,}8A}{f^*}\left(\frac{u_0 l}{\nu_0}\right)^{-0,2} = \frac{0{,}8A}{f^*}\,\mathrm{Re}^{-0,2}, \tag{22}$$

where we find $\delta^*(\ell)/\ell$ from (20).

We shall assume that (22) is also valid for a liquid fluidized bed. The cofactor in the braces in the second term of (17), with allowance for (22) and the relations $a = k\ell u$ and $\delta^* = f^*\delta$, is reduced to the form

$$\left(\frac{u\delta}{a}\,\frac{\partial\delta}{\partial x}\right) = \frac{0{,}8}{kf^{*^2}}\left(\frac{\delta^*}{l}\right)^2 = \frac{0{,}8A^2}{kf^{*^2}}\,\mathrm{Re}^{-0,4} = \\ = \frac{(1-m)\,c^2}{f^{*^2}}\,\mathrm{Re}^{-0,4}, \quad c^2 = \frac{0{,}8A^2}{(1-m)\,k}, \tag{23}$$

where $\delta^* = \delta^*(\ell)$.

Substituting (19) and (23) into (17), we obtain

$$\frac{\partial^2 T}{\partial\eta^2} + \frac{(1-m)\,c^2}{f^{*^2}}\,\mathrm{Re}^{-0,4}\eta\,\frac{\partial T}{\partial\eta} + \frac{m}{\eta}\,\frac{\partial T}{\partial\eta} = 0. \tag{24}$$

The thermal-flux density with passage to η can be written as follows:

$$q = -\rho_0 c_0 \vartheta_0\,\frac{a}{\delta}\left(\frac{\partial T}{\partial\eta}\right)_w; \quad \mathrm{St} = -k\left(\frac{l}{\delta}\right) f(\eta)\left(\frac{\partial T}{\partial\eta}\right)_w. \tag{25}$$

Extending the coordinate $\eta = \xi/\mathrm{St}$, we convert (24) to the form

$$\mathrm{St}^2\left\{\frac{\partial T}{\partial\xi}\right\} + \frac{(1-m)c^2}{f^{*^2}}\,\mathrm{Re}^{-0,4}\left\{\frac{\partial T}{\partial\xi}\right\} + m\,\mathrm{St}^2\left\{\frac{1}{\zeta}\,\frac{\partial T}{\partial\zeta}\right\} = 0. \tag{26}$$

Equating the expressions in the braces to constants (± 1), we obtain an equation for the average Stanton number:

$$f^{*^2}\,\mathrm{St}^2 = c^2\,\mathrm{Re}^{-0,4}, \quad c^2 = \frac{0{,}8A^2}{(1-m)\,k}. \tag{27}$$

If as the function $f^*(\mathrm{Pr})$ we use $f^*(\mathrm{Pr}) = \mathrm{Pr}^{0,4}$ [9], Eq. (27) takes the form

$$\mathrm{St}\,\mathrm{Pr}^{0,4} = c\,\mathrm{Re}^{-0,2}. \tag{28}$$

To allow for the effect on heat exchange of the passage of bubbles through the bed, we use (1):

$$\mathrm{St}_\beta = c\,\mathrm{Re}^{-0,2}\,\mathrm{Pr}^{-0,4}\left(\frac{\beta}{1-\beta}\right)^{1/12}. \tag{29}$$

It should be noted that this same result can be obtained if a term D(1) for the convective dispersion due to bubbling through is added to the expression for the thermal-diffusivity coefficient.

Considering that $(\beta/(1-\beta))^{1/12} \approx \beta^{0,1}$, we convert in (29) to Nusselt numbers ($\mathrm{Nu} = \mathrm{StPe} = \mathrm{StRePr}$):

$$\mathrm{Nu} = c\,\mathrm{Re}^{0,8}\,\mathrm{Pr}^{0,6}\,\beta^{0,1}. \tag{30}$$

The constant c and the exponents are subject to correction on the basis of experimental data, since there are no analytic solutions of the problem in question.

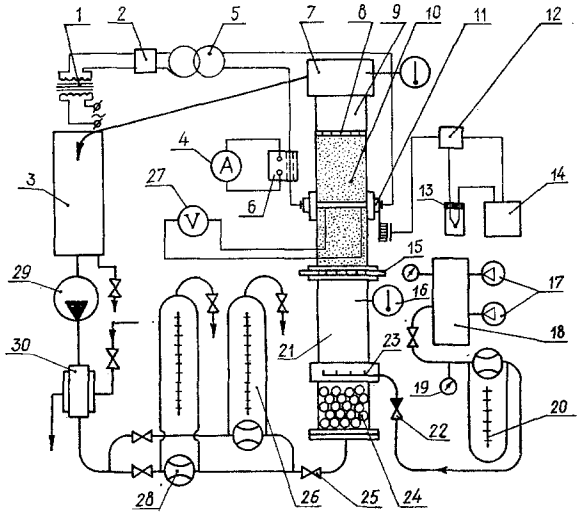

Fig. 2. Experimental setup. 1) RNO-250-5 autotransformer; 2) K-50 measuring set; 3) collecting tank; 4) ammeter; 5) TS-50 transformer; 6) current transformer; 7) expansion chamber; 8) piston; 9) working channel; 10) gas–liquid fluidized bed; 11) experimental section with electrocalorimeter; 12) PMT-20 switch; 13) Dewar flask; 14) F-30 measuring set; 15) support and separating grating; 16) thermometer; 17) compressor; 18) receiver; 19) pressure gauge; 20) U-tube differential gauge; 21) hydrodynamic-stabilization channel; 22) return channel; 23) bubbler; 24) mixing chamber; 25) valve; 26) П-tube differential gauge; 27) digital voltmeter; 28) flowmeter diaphragm; 29) pump; 30) cooler.

Experiments were performed using the setup shown in Fig. 2 to check the model representations of the mechanism of heat exchange in a three-phase fluidized bed.

A bed of granular material was fluidized in a vertical channel with a rectangular cross section of 50 × 140 mm and a height of 1000 mm. The experimental section was preceded by a section of hydrodynamic stabilization, between which was installed a perforated grating covered by a fine-mesh metal screen to prevent the granular material from falling through the grating. The fluidizing medium was a mixture of air with water and aqueous solutions of glycerin. The liquid was circulated through a closed circuit, while the gas channel had an open circuit. Coaxial openings for an electrocalorimeter were made in sleeves on the side walls of the channel at a certain distance from the perforated grating along the height of the experimental section. Electrocalorimeters with outside diameters of 6 and 16 mm were used in the experiments. The air was mixed with the liquid in a chamber of rectangular cross section with a bubbler installed in it. To obtain a homogeneous mixture of air and liquid, the openings through which the air was sprayed were arranged uniformly with identical spacings.

The quantitative effect of the determining similarity criteria Re, Pr, and β obtained theoretically in Eq. (30) was confirmed by analysis of experimental data on the heat exchange of a horizontal cylinder placed in a bed of particles fluidized by a mixture of water and air. As a result of processing of these data, a correction was made in the exponents of the determining similarity criteria and the proportionality factor c was determined. The generalizing experimental dependence of the heat exchange of a horizontal cylinder with a gas–liquid fluidized bed has the form

$$\mathrm{Nu} = 0{,}14\,\mathrm{Re}^{0{,}75}\,\mathrm{Pr}^{0{,}63}\beta^{0{,}1}\varepsilon_q, \qquad (31)$$

where $\varepsilon_q = (\mathrm{Pr}_0/\mathrm{Pr}_w)^{0{,}25}$ is a correction for the direction of the thermal flux in a system that has a liquid phase.

The determining parameters in (31) are the equivalent diameter of a pore channel, $\ell = d_e = (2/3)(\varepsilon/1-\varepsilon)d$, the liquid velocity $u_0 = u_{f0}/\varepsilon$, and the mixture temperature. Therefore,

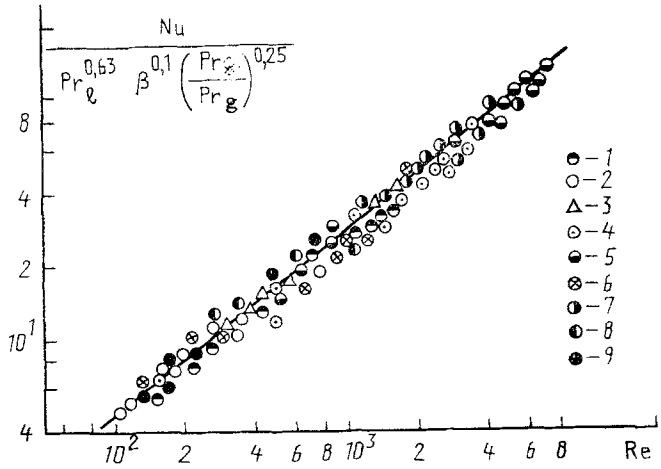

Fig. 3. Generalization of experimental data for stabilized heat exchange of horizontal cylinder in gas–liquid boiling bed: water–air–glass (1) d = 0.78 mm, 2) 0.91, 3) 1.34; 4) 3.17; 5) 3.61); alundum (6) 1.38; 7) 2.97); 20% glycerin solution–air–glass (8) 2.36); alundum (9) 0.95); the line represents Eq. (31).

$$\mathrm{Nu} = \frac{\alpha d_e}{\lambda_0};\quad \mathrm{Re} = \frac{u_0 d_e}{\nu_0} = \frac{u_{f0} d_e}{\varepsilon \nu_0};\quad \beta = \frac{u_{fg}}{u_{f0} + u_{fg}}. \tag{32}$$

Equation (31) is valid in the following ranges of determining similarity criteria: Re = 200-6200, Pr = 5-20, and β = 0.05-0.4. A graphical representation of generalizing relation (31) is provided in Fig. 3.

Thus, as the mechanisms of heat transfer in a gas–liquid fluidized bed are determined more precisely, the approaches examined here will provide fairly simple and accurate formulas for calculation of processes of heat transfer to various heat-exchange surfaces.

NOTATION

x and y are coordinates; T and ϑ are the dimensionless and excess temperatures, which are defined in (2); $\hat{a}$ and $\hat{\lambda}$ are the thermal-diffusivity and thermal-conductivity tensors; $\rho_0 c_0$ is the volume specific heat of the liquid; D, a, and λ are the coefficients of convective dispersion, thermal diffusivity, and thermal conductivity; α is the heat-exchange coefficient; $u(u_x, u_y)$ is the liquid-velocity vector and its components; R, a, d, ℓ, and L are the radii of the cylinder and particles, the particle diameter, the characteristic microscale, and the length of the plate; γ is a parameter in (6); k_D, k_S, k_q, k, A, c_S, and c are proportionality factors in (1), (2), (3), (4), (6), (20), and (23); δ* and δ are the thicknesses of the hydrodynamic and thermal boundary layers; m is the exponent of the velocity distribution in the boundary layer; f*(Pr) is a function that relates δ* and δ; β is the gas concentration by volume in (32); ε is the average porosity through the volume of the bed; St, Pe, Pr, Re, and Nu are the Stanton, Péclet, Prandtl, Reynolds, and Nusselt numbers; ξ, ζ, and η are variables in (9), (16), and (17). Subscripts: 0) liquid phase; q) gas; w) heat-heat-exchange surface; and f) filtration.

LITERATURE CITED

1. I. G. Malenkov, Prikl. Mekh. Tekh. Fiz., No. 2, 130-134 (1968).
2. L. K. Vasanova, A. P. Polozov, and G. P. Yasnikov, Inzh.-fiz. Zh., 55, No. 5, 784-788 (1988).
3. Yu. A. Buevich and D. A. Kazenin, Prikl. Mekh. Tekh. Fiz., No. 5, 94-102 (1977).
4. Yu. A. Buevich and E. B. Perminov, Inzh.-fiz. Zh., 40, No. 2, 254-263 (1981).
5. V. V. Dil'man and A. D. Polyanin, Model-Equation and Analogy Methods [in Russian], Moscow (1988).
6. N. N. Kochin, I. A. Kibel', and N. V. Roze, Theoretical Hydromechanics [in Russian], Moscow (1953).
7. Yu. A. Buevich, D. A. Kazenin, and N. N. Prokhorenko, Inzh.-fiz. Zh., 29, No. 3, 410-418 (1975).

8. T. Sebisi and P. Bradshaw, Convective Heat Exchange [Russian translation], Moscow (1987).
9. S. Sou, Hydrodynamics of Multiphase Systems [Russian translation], Moscow (1971).

EFFECT OF ELEVATED CARRIER-GAS PRESSURE ON HYDRAULIC CHARACTERISTICS OF GAS–SOLID PARTICLE TWO-PHASE FLOW

V. I. Timoshenko, Yu. V. Knyshenko, V. F. Kopysov, and E. N. Gromov

UDC 532.529

The effect of elevated gas pressure on the hydraulic resistance and critical velocity of a two-phase flow is studied on a pneumatic-transport bench. It is established that for each working-pressure level there exists a limiting solid-phase concentration, the exceeding of which causes an abrupt rise in hydraulic resistance.

Gas flows in pipes in the presence of a disperse phase in the form of solid particles take place in various technological processes: in power engineering mining, the chemical industry, and metallurgy. Such flows are typical in practice in the pneumatic transport of granular materials, which is gaining wider use in the indicated areas.

Pneumatic transport is being developed to increase the concentration of granular material in the pipe and the transport distance, which makes it necessary to increase the carrier-gas pressure.

Preliminary estimates show that granular loads can be carried distances of from 1-2 to several tens of kilometers through a pneumatic-transport line (for example, coal, ore, and other raw materials from the production site to the consumer). The working gas pressures at the beginning of the pipe will be within 0.5 to 3-4 MPa.

The accumulated experimental material on two-phase flows [1-11], which has been generalized in the form of dependences for hydraulic resistances, critical velocities, sliding velocities, acceleration parameters, and other quantities, was obtained at small working pressures (0.1-0.2 MPa). The use of these results in the design of systems with increased carrier-gas pressure requires proper substantiation.

We studied the effect of an increase in gas pressure (to 1.4 MPa) on such hydraulic characteristics of two-phase flow as hydraulic resistance, critical velocity, and sliding velocity.

1. The study was performed on a pneumatic-transport bench, a diagram of which is shown in Fig. 1.

The bench is mounted in a closed scheme with two circuits: one for the pure gas and one for the two-phase suspension. The bench includes two series-connected circulation units (CU), which consist of spur-gear compressors of type 2AF51É52Sh in sealed enclosures, which are filled with gas simultaneously with the pneumatic-transport pipes. The noncirculating part of the bench consists of transport pipes with horizontal measuring sections and loading and unloading devices. The noncirculating part is filled with gas to the working pressure from a gas-supply unit with a bank of high-pressure cylinders (p_w = 15 MPa) and a system for controlling and monitoring the output pressure.

The loading device (LD) is a cyclone unit mounted on a cylindrical hopper, in whose lower part is a variable-speed drum feeder. The unloading device (UD) consists of a cyclone and a receiving hopper.

Institute of Engineering Mechanics, Academy of Sciences of the Ukraine, Dnepropetrovsk.
Translated from Inzhenerno-fizicheskii Zhurnal, Vol. 62, No. 2, pp. 188-194, February, 1992. Original article submitted April 9, 1991.

 1062-0125/92/6202-0134$12.50